Avrupa Bilim ve Teknoloji Dergisi
Özel Sayı 28, S. 1366-1371, Kasım 2021

Araştırma Makalesi

www.ejosat.com ISSN:2148-2683

European Journal of Science and Technology
Special Issue 28, pp. 1366-1371, November 2021

Research Article

Investigation of Normalization Values of S-Parameters in Microstrip Antenna Structure in Pathological Tissue Samples

Rabia Toprak[1*], Seyfettin Sinan Gültekin[2], Dilek Uzer[2]

[1*] Karamanoğlu Mehmetbey University, Faculty of Engineering, Departmant of Electrical-Electronics Engineering, Karaman, Turkey, (ORCID: 0000-0002-3306-1163), rabiatop@kmu.edu.tr

[2] Konya Technical University, Faculty of Engineering and Nature Sciences, Departmant of Electrical-Electronics Engineering, Konya, Turkey, (ORCID: 0000-0002-6287-9124, 0000-0003-3850-3810), ssgultekin@ktun.edu.tr, duzer@ktun.edu.tr

(1st International Conference on Applied Engineering and Natural Sciences ICAENS 2021, November 1-3, 2021)

(**DOI:** 10.31590/ejosat.1017084)

ATIF/REFERENCE: Toprak, R., Gültekin, S. S. & Uzer, D. (2021). Investigation of Normalization Values of Microstrip Antenna Structure and S-Parameters in Pathological Tissue Samples. *European Journal of Science and Technology*, (28), 1366-1371.

Abstract

Studies on the examination of pathological tissue samples with antennas have begun to be developed. In this study, normalization studies performed using a microstrip antenna structure with increased gain are presented. FR-4 substrate with a dielectric constant of 4.4 is preferred in the antenna structure used in the normalization studies. In pathological tissue samples, samples of normal and cancerous skin tissue are modeled in HFSS and simulated. The differences in the normalized S-parameters as a result of the simulations are shown in the tables. While the normal skin tissue normalization value at S_{11} is 13.4, the value for the tumor skin tissue sample is 18.0. For other S-parameters, different values are obtained for normal and cancerous skin tissue. The differences in the values reveal the success of the proposed antenna structure.

Keywords: Pathology, Microstrip, Patch, Normalization, HFSS.

Patolojik Doku Örneklerinde Mikroşerit Anten Yapısında S-Parametrelerine Ait Normalizasyon Değerlerinin İncelenmesi

Öz

Patolojik doku örneklerinin antenlerle incelenmelerine ait çalışmalar geliştirilmeye başlanmıştır. Bu çalışmada kazancı artırılmış bir mikroşerit anten yapısı kullanılarak gerçekleştirilen normalizasyon çalışmaları sunulmaktadır. Normalizasyon çalışmalarında kullanılan anten yapısında 4.4 dielektrik sabiti değerine sahip FR-4 taban tercih edilmiştir. Patolojik doku örneklerinde normal ve kanserli deri dokusuna ait numuneler HFSS'de modellenerek simülasyonları yapılmıştır. Yapılan simülasyonlar sonucunda normalize edilen S-parametrelerindeki farklılıklar tablolar ile gösterilmiştir. S_{11} değerindeki normal deri dokusu normalizasyon değeri 13.4 iken, tümörlü deri dokusu örneğine ait değer 18.0 olarak bulunmuştur. Diğer S-parametreleri için de normal ve kanserli deri dokusu için farklı değerler elde edilmiştir. Değerlerdeki farklılıklar tasarlanan anten yapısının başarısını ortaya koyaktadır.

Anahtar Kelimeler: Patoloji, Mikroşerit, Yama, Normalizasyon, HFSS.

[*] Corresponding Author: rabiatop@kmu.edu.tr

1. Introduction

Pathology is derived from the ancient Greek term 'pathos' meaning disease and is used to mean the scientific study of diseases. In a broader sense, pathology examines the causes of diseases, the way they affect tissues and organs, especially the morphological (formal, visual) features of diseased tissues and organs. In this sense, pathology forms the basis of medicine. Pathology; It provides an easier understanding of diseases by adding the abnormal appearance of diseased organs with the naked eye or under the microscope to the knowledge learned in anatomy and physiology. In areas where appearances are very helpful in decision making, the contribution of pathological examination to the diagnosis and determination of the appropriate treatment method is also very great. Today, pathological examination is necessary and obligatory for the definitive diagnosis of many diseases, especially the diagnosis of tumors (Kamel, 2011; Nakhleh, 2006; Patterson, 2014).

A pathologist tries to diagnose diseases by examining samples taken in various forms from tissues and organs that are thought to be diseased. The routinely used method for this is microscopic examination. Most of the pathologist's time is spent examining tissues with the naked eye and microscope and preparing reports for these examinations. The tissue of the organ removed from the body is placed in a fixing fluid called formal. 2-5 µm of this liquid is cut and placed on the surface of the slide for microscopic examination. The dimensions of the slide are 26x76x1 mm^3. The tissue fixed to the slide is covered with paraffin blocks and stored for the evaluation part (Patterson, 2014). The evaluation period is important for the patient and doctor waiting for the report result. Sometimes it can take months to reach the pathological results reports. For this reason, various studies are included in order to shorten this period.

Antenna applications in biomedical area are gained acceleration(Caccami, Hogan, Alfredsson, Marrocco, & Batchelor, 2018; Chow, Ouyang, Beier, Chappell, & Irazoqui, 2009; Hong, Choi, Magill, Shah, & Felder, 2018; Lin, Chen, & Yen, 2018; Meredov, Klionovski, & Shamim, 2019). Especially microstrip patch antenna structure is one of the most researched topics in the medical applications because of several advantages (Hasan, Shanto, Howlader, & Jahan, 2018; Lane, Biondi, JS Pleva - US Patent 5, & 1995, n.d.; Mak, C.L. and Luk, K.M. and Lee, K.F. and Chow, 2000; Nalam, Rani, & Mohan, 2014; Singh & Tripathi, 2011; Top, 2017). These are low-profile, cost, small dimensions, ease of design and weight. Low gain, efficiency and impedance matching are some disadvantages of microstrip patch antenna types (Dey & Mittra, 1996; Lane et al., n.d.).

Microstrip patch antenna structures have been started to be investigated in order to detect pathological tissue samples. It is aimed to shorten the access time to reports by using antenna structures. Thus, it will be possible to access the pathological results reports in a short time, especially for life-threatening patients.

In this study, microstrip patch antenna with previously increased gain from 1.89 dB to 3.50 dB was used. The antenna structure was simulated and tested on the modeled system. The modeled system includes pathological tissue samples placed equidistantly between two identical antenna structures. The electrical values of normal and cancerous skin tissue were introduced to ANSYS HFSS program and simulations were made. S-parameter values were obtained as a result of simulations. The differences between normal and cancerous skin tissue were shown by normalization from these values. Normalization in electronics is the comparison of a value to a reference. In other words, it is keeping the data within its limits without changing the relationship between the variables. It is a characterization method used for electrical and electronic based systems in the literature (Alexander, Klavsuts, Klavsuts, & Khayrullina, 2016; Jin et al., 2016).

Section 2 explains the Material and Method part. Results and Discussions are in Section 3. Finally, Conclusion part is in Section 4.

2. Material and Method

2.1. Antenna Structure

Antenna operating frequency ise selected 2.45 GHz because of ISM (Industrial, Scientific and Medical) bands. As substrate material is used FR-4 that has 4.4 dielectric constant value. Antenna dimensions are obtained from Equations 2.1 and 2.2 (B. J. Kwaha, O. N. Inyang, 2011). For finding the resonance frequency, lots of simulations are implemented. After simulations, substrate dimension is found 38.3x38.3x1.575 mm^3. Proposed antenna patch structure is obtained by combining a concentric circle with a diameter of 28.84 mm and 4 concentric circles with a diameter of 16 mm and 4 concentric circles with a diameter of 14 mm at the same distance from the center. Figure 1 shows the antenna structure. Return loss of the proposed antenna is showed in Figure 2. Gain graph is in Figure 3.

$$a = \frac{F}{\{1+\frac{2h}{\pi\varepsilon_r F}\left[\ln\left(\frac{\pi F}{2h}\right)+1.7726\right]\}^{\frac{1}{2}}} \qquad (2.1)$$

$$F = \frac{8.971x10^9}{f_r\sqrt{\varepsilon_r}} \qquad (2.2)$$

Where, a is radius of the circular patch, f_r is resonance frequency, ε_r is dielectric constant of substrate and h is height of substrate.

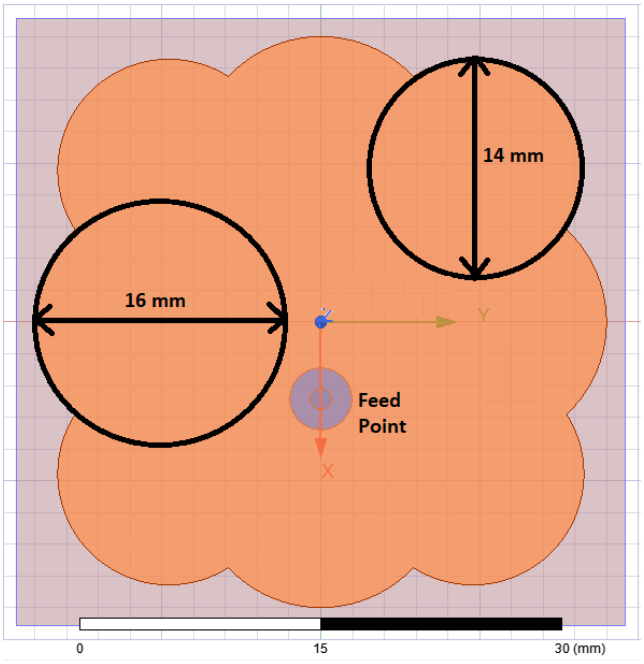

Figure 1. Proposed antenna structure and its dimensions

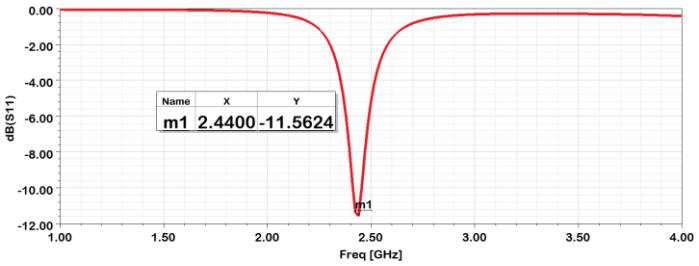

Figure 2. Return Loss of the antenna structure

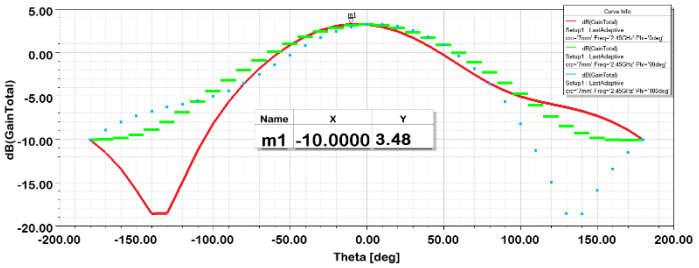

Figure 3. Gain value of the antenna structure

2.2. Modeled System

Each tissue part of the human body part has a different electrical value. These values align permittivity, permeability and conductivity. In the literature, there is a study to measure the electrical properties of body part (Gabriel, 1996). So, the electrical values of normal and cancerous skin tissue are introduced to the HFSS program. Normal skin dielectric constant is 38, while cancerous skin dielectric constant value is 50.

Modeled system is shown in Figure 4. For simulations, two identical antenna structures at equal distance of 25 mm are used in the system. 25 mm is used because of far-field region (Equation 2.3) (Balanis, 2013). Also, between two antenna structures, there are pathological tissue samples. In the center, there is a glass slide ($26x76x1$ mm^3) that fixed skin tissue samples. These samples are spread on the glass to cover the entire slide. Height of samples is 5 µm.

$$r > \frac{2d^2}{\lambda} \quad (2.3)$$

Where r is the far field distance, d is the maximum linear dimension of the antenna and λ is the operating wavelength. The reason for choosing the far field is that the operations take place at the free space impedance (Bansal, 1999).

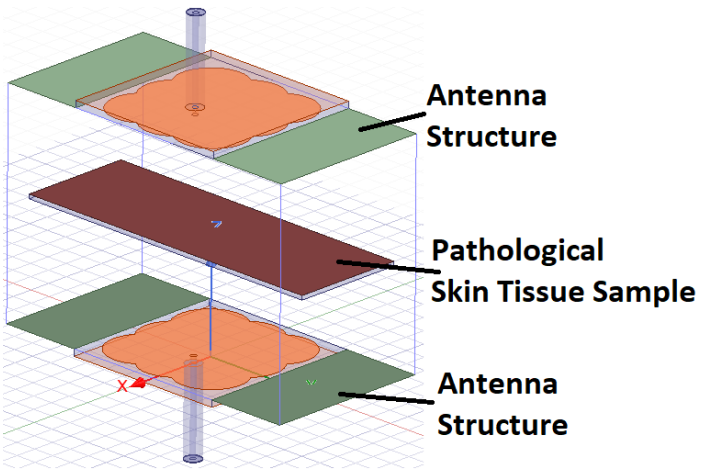

Figure 4. Modeled system structure

2.3. Normalization Definition

The principle of normalization is to compare variables with each other. Normalization is done differently depending on the level of measurement of the variables, and is intimately related to the uniqueness properties of the measurement level (Aguinis et al., 2019).

In this work, it is aimed to obtain differences from S-parameters, S_{11}, S_{21}, S_{12} and S_{22}. These parameters are important to explain the radiation values of the antenna structure (Caspers, 2011). They express the return loss and transmission loss of the antenna structure. Here, as shown in Figure 4, firstly while there is no glass slide, simulations are done and saved. Then while there is only empty glass slide, simulations are done and saved. These data are S-parameters (Alhuwaidi et al., 2015; Ghodgaonkar, Varadan, & Varadan, 1989). each value is divided by the value in the same state as it (Figure 5). Equation 2.4 explains this situation.

$$\frac{(S_{ij})_{empty\ glass\ slide}}{(Sij)_{air}} \quad i,j = 1,2,\ldots \quad (2.4)$$

Where S_{ij} expresses the value of S-parameters (for i,j=1,2). This ratio uses to obtain the differences of both normal skin and cancerous skin tissue. Then while there is normal skin tissue on glass slide, simulations are done and saved. Afterwards, the same process is performed in cancerous skin tissue. The value obtained for both tissue types is divided by the above ratio. Equations 2.5 and 2.6 explain that (Figure 6).

$$\frac{(S_{ij})_{normal\ skin\ tissue}}{\frac{(S_{ij})_{empty\ glass\ slide}}{(Sij)_{air}}} \quad i,j = 1,2,\ldots \quad (2.5)$$

$$\frac{(S_{ij})_{cancerous\ skin\ tissue}}{\frac{(S_{ij})_{empty\ glass\ slide}}{(Sij)_{air}}} \quad i,j = 1,2,\ldots \quad (2.6)$$

For normal and cancerous skin tissues, obtained values compare with each other and the differences are evaluated.

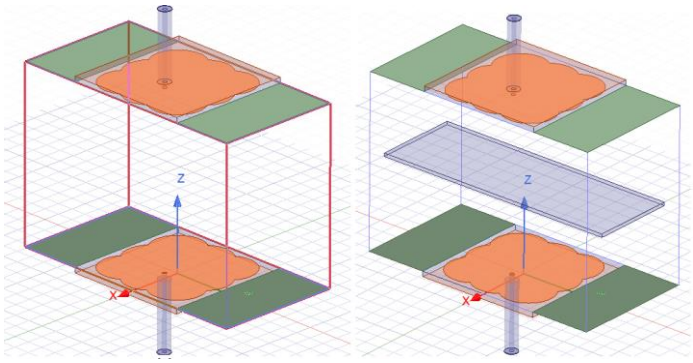

Figure 5. Modeled system for normalizations with empty and glass slide

3. Results and Discussion

Firstly, obtained values are in dB. So, these are converted to the unitless values. Then the proportions are made.

The graphs given in between Figure 7 and Figure 10 show the normalization graphs of the normal and cancerous skin tissue of the S-parameters. When Figure 7 is examined, it is seen that the normalization differences are maximum at S_{11} values, especially at 8.6 GHz. Here, the value obtained for the skin tissue is 13.4, while the value of the cancerous tissue is 18.0.

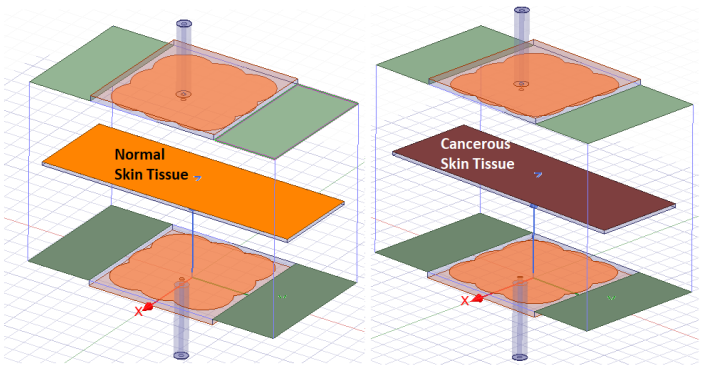

Figure 6. Modeled system for normalizations with normal and cancerous skin tissue

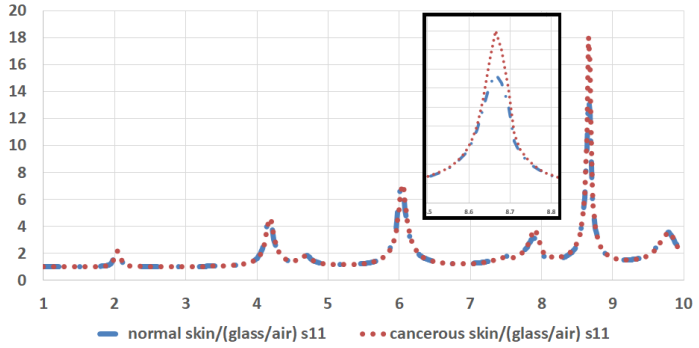

Figure 7. Normalization graph for S_{11} values

When Figure 8 is examined, it is seen that the difference between S_{21} values and 4.6 GHz is maximum. While the normalization value of skin tissue is 750, the value of cancerous tissue is 560.

In Figure 9, the S_{12} values, again at 4.6 GHz frequency values, are 561 for the skin, while the value obtained from the maximum normalization is 461 for the cancerous skin tissue.

When Figure 10 is examined, S_{22} values, while the maximum value for skin tissue is 33.5 in the 8.6 GHz region, this value is 24.9 for cancerous tissue.

In Figure 11, the differences of normalization values obtained from normal and cancerous skin tissues vary according to frequency. Here, the difference graph using the equation of the data (normal skin-cancerous skin) shown in Figures 7-10 is shown. The importance of this graph (Figure 11) is very important in terms of showing the difference sizes. At 4.6 GHz, the skin-tumor difference is 557.3 maximum for S_{21}, while the maximum difference value for S_{12} is 446.0.

When the size of the difference between normal and cancerous skin tissue from the obtained S-parameter values is examined, it is possible to interpret as follows:

• Difference and change rates in the 4.6 GHz region are especially important for S_{21} and S_{12} values. This frequency region is ideal for differential detection.

• The 8.6 GHz frequency region is important in processing the values given by the transmitting and receiving antennas. The band where the reflection coefficients are effective is in this range.

• In particular, the difference region of the S_{21} value, which gives the transmission coefficient, is located around the 4.6 GHz band. The magnitude data of the difference value, which can be clearly seen in Figure 8, will play an active role in the future of the researches.

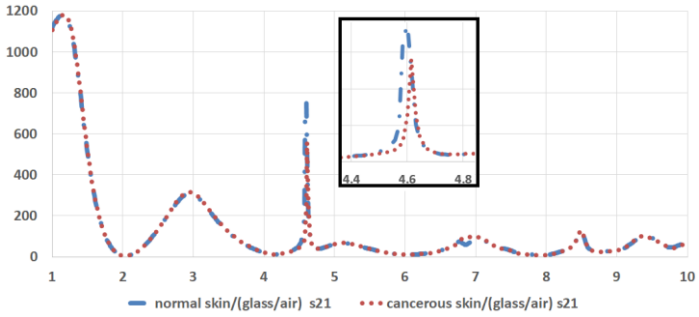

Figure 8. Normalization graph for S_{21} values

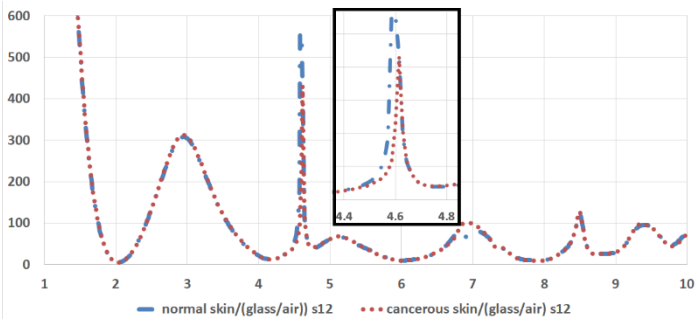

Figure 9. Normalization graph for S_{12} values

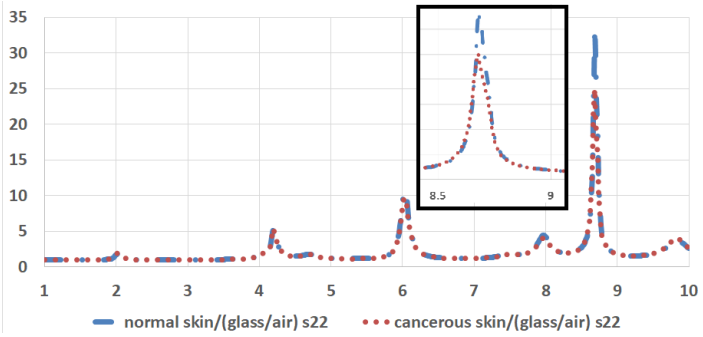

Figure 10. Normalization graph for S_{22} values

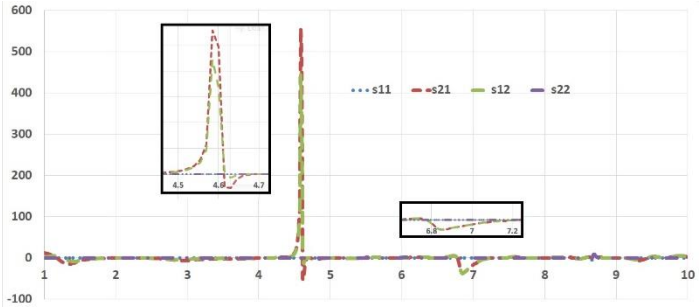

Figure 11. Comparison graph of the differences of the data of the S-parameters (normal skin-cancerous skin)

4. Conclusion

Pathology, the branch of science that examines the data of the tissues, contains important information about the patient and the disease with its prepared reports. Reaching these reports can sometimes take months, depending on the number of patients and samples.

Microstrip patch antenna designs were investigated in order to shorten the time to reach the reports for the patient and the doctor. These antenna structures are frequently used in the literature. An antenna structure with a gain of about 3.5 dB relative to a microstrip patch was chosen.

On the other hand, the difference between normal and cancerous skin tissue was shown by normalization on the S-parameters containing the radiation information of the antennas. For example, when S_{11} normalization values were examined, 13.4 was obtained for normal skin tissue and 18.0 for cancerous skin tissue. S_{21}, which is especially important because it contains transmission information, is 750 for normal skin tissue and 560 for cancerous skin tissue. In systems where antennas are used, these differences aim to provide report information to doctors in a short time, especially for patients with vital importance. When the graphs and values are examined, the success of the antenna structures and the selected antenna structure for the modeled study is shown.

5. Acknowledge

This study is supported by Konya Technical University Scientific Research Projects Coordinatorship with project number 211102032.

References

Aguinis, H., Bailey, J. R., Borgatti, S. P., Boyd, B., DeJordy, R., DeSimone, J. A., … Schurer Lambert, L. (2019). Recommendations for Improved Methods and Analysis in Management Research. *Academy of Management Proceedings*, *2019*(1), 17367. https://doi.org/10.5465/AMBPP.2019.17367SYMPOSIUM

Alexander, G., Klavsuts, I. L., Klavsuts, D. A., & Khayrullina, M. V. (2016). AC voltage normalization - Conception and technology for smart grid system. *Proceedings - 2016 51st International Universities Power Engineering Conference, UPEC 2016*, *2017-Janua*, 1–5. https://doi.org/10.1109/UPEC.2016.8114115

Alhuwaidi, S., Zubair, K., Song, H., Shellman, Y., Robinson, W., & Robinson, S. (2015). Disease diagnostics of biological tissues using free-space technique in terahertz frequency range. *IEEE Biomedical Circuits and Systems Conference: Engineering for Healthy Minds and Able Bodies, BioCAS 2015 - Proceedings*. https://doi.org/10.1109/BioCAS.2015.7348378

B. J. Kwaha, O. N. Inyang, P. A. (2011). The circular microstrip patch antenna-design and implementation. *International Journal of Recent Research and Applied Studies (IJRRAS)*, *8*(1), 86–95.

Balanis, C. A. (2013). *Anten teorisi : analiz ve tasarım*. Nobel Akademik Yayıncılık.

Bansal, R. (1999). The far-field: How far is far enough? *Applied Microwave and Wireless*, *11*(11), 58–60.

Caccami, M. C., Hogan, M. P., Alfredsson, M., Marrocco, G., & Batchelor, J. C. (2018). A Tightly Integrated Multilayer Battery Antenna for RFID Epidermal Applications. *IEEE Transactions on Antennas and Propagation*, *66*(2), 609–617. https://doi.org/10.1109/TAP.2017.2780899

Caspers, F. (2011). RF engineering basic concepts: S-parameters. *CAS 2010 - CERN Accelerator School: RF for Accelerators, Proceedings*, (June), 67–93.

Chow, E. Y., Ouyang, Y., Beier, B., Chappell, W. J., & Irazoqui, P. P. (2009). Evaluation of cardiovascular stents as antennas for implantable wireless applications. *IEEE Transactions on Microwave Theory and Techniques*, *57*(10), 2523–2532. https://doi.org/10.1109/TMTT.2009.2029954

Dey, S., & Mittra, R. (1996). Compact microstrip patch antenna. *Microwave and Optical Technology Letters*, *13*(1), 12–14. https://doi.org/10.1002/(sici)1098-2760(199609)13:1<12::aid-mop4>3.0.co;2-q

Gabriel, C. (1996). Compilation of the Dielectric Properties of Body Tissues at RF and Microwave Frequencies. *Environmental Health*, *Report No.*(June), 21. https://doi.org/Report N.AL/OE-TR- 1996-0037

Ghodgaonkar, D. K., Varadan, V. V., & Varadan, V. K. (1989). A Free-Space Method for Measurement of Dielectric Constants and Loss Tangents at Microwave Frequencies. *IEEE Transactions on Instrumentation and Measurement*, *38*(3), 789–793. https://doi.org/10.1109/19.32194

Hasan, R. R., Shanto, M. A. H., Howlader, S., & Jahan, S. (2018). A novel design and miniaturization of a scalp implantable circular patch antenna at ISM band for biomedical application. *2017 Intelligent Systems Conference, IntelliSys 2017*, *2018-Janua*(September), 166–169. https://doi.org/10.1109/IntelliSys.2017.8324286

Hong, S. M., Choi, C. H., Magill, A. W., Shah, N. J., & Felder, J. (2018). Design of a Quadrature 1H/31P Coil Using Bent Dipole Antenna and Four-Channel Loop at 3T MRI. *IEEE Transactions on Medical Imaging*, *37*(12), 2613–2618. https://doi.org/10.1109/TMI.2018.2844462

Jin, H. S., Choi, B. H., Kang, J. K., Kim, S. I., Lim, J. H., & Song, S. Y. (2016). Measurement and Normalization Methods to Provide Detailed Information on Energy Consumption by Usage in Apartment Buildings. *Energy Procedia*, *96*(October), 881–894. https://doi.org/10.1016/j.egypro.2016.09.161

Kamel, H. M. (2011). *Trends and Challenges in Pathology Practice Choices and necessities*. *11*(1), 38–44.

Lane, J., Biondi, J., JS Pleva - US Patent 5, 400,040, & 1995, undefined. (n.d.). Microstrip patch antenna. In *Google Patents*. Retrieved from https://patents.google.com/patent/US5400040A/en

Lin, J. Y., Chen, H. C., & Yen, M. Y. (2018). Sensor/Antenna Interface IC for Implantable Biomedical Monitoring System. *IEEE Transactions on Microwave Theory and Techniques*, *66*(3), 1660–1667. https://doi.org/10.1109/TMTT.2017.2755647

Mak, C.L. and Luk, K.M. and Lee, K.F. and Chow, Y. . (2000). Experimental study of a microstrip patch antenna with an L-shaped probe. *IEEE Transactions on Antennas and Propagation*, *48*, 777–783.

Meredov, A., Klionovski, K., & Shamim, A. (2019). Screen-Printed, Flexible, Parasitic Beam-Switching Millimeter-Wave Antenna Array for Wearable Applications. *IEEE Open Journal of Antennas and Propagation*, *1*, 2–10. https://doi.org/10.1109/OJAP.2019.2955507

Nakhleh, R. E. (2006, July 1). What is quality in surgical pathology? *Journal of Clinical Pathology*, Vol. 59, pp. 669–672. https://doi.org/10.1136/jcp.2005.031385

Nalam, M., Rani, N., & Mohan, A. (2014). Biomedical Application of Microstrip Patch Antenna. *International Journal of Innovative Science and Modern Engineering (IJISME)*, *2*(6), 6–8.

Patterson, J. (2014). *Weedon's Skin Pathology E-Book* (Fourth).

Retrieved from https://www.google.com/books?hl=tr&lr=&id=Y-LTBQAAQBAJ&oi=fnd&pg=PP1&dq=patterson+2014+pathology&ots=U3wha_QPa1&sig=0fYB8PC-f3bX5-UQ0robmQaUhFY

Singh, I., & Tripathi, V. S. (2011). Micro strip Patch Antenna and its Applications: a Survey. In *Article in International Journal of Computer Applications in Technology*. Retrieved from https://www.researchgate.net/publication/232318276

Top, R. (2017). *A transmitter microstrip antenna design and application towards the detection of heart disease parameters*. Selcuk University.